



Published in final edited form as:

*J Refract Surg.* 2008 June ; 24(6): 571–581.

## Epithelial Thickness in the Normal Cornea: Three-dimensional Display With Very High Frequency Ultrasound

Dan Z. Reinstein, MD, MA(Cantab), FRCSC, Timothy J. Archer, MA(Oxon), DipCompSci (Cantab), Marine Gobbe, MST(Optom), PhD, Ronald H. Silverman, PhD, and D. Jackson Coleman, MD

London Vision Clinic, London (Reinstein, Archer, Gobbe); the Department of Ophthalmology, St Thomas' Hospital, Kings College, London, United Kingdom (Reinstein); the Department of Ophthalmology, Weill Cornell Medical College, Ithaca, NY (Reinstein, Silverman, Coleman); Centre Hospitalier National d'Ophthalmologie, Paris, France (Reinstein); and Riverside Research Institute, New York, NY (Silverman)

### Abstract

**PURPOSE**—To characterize the in vivo epithelial thickness profile in a population of normal eyes.

**METHODS**—An epithelial thickness profile was measured by Artemis 1 (Ultralink LLC) very high-frequency (VHF) digital ultrasound scanning across the central 10-mm diameter of the cornea of 110 eyes of 56 patients who presented for refractive surgery assessment. The average, standard deviation, minimum, maximum, and range of epithelial thickness were calculated for each point in the 10×10-mm Cartesian matrix and plotted. Differences between the epithelial thickness at the corneal vertex and peripheral locations at the 3-mm radius were calculated. The location of the thinnest epithelium was found for each eye and averaged. Correlations of corneal vertex epithelial thickness with age, spherical equivalent refraction, and average keratometry were calculated.

**RESULTS**—The mean epithelial thickness at the corneal vertex was 53.4±4.6 μm, with no statistically significant difference between right and left eyes, and no significant differences in age, spherical equivalent refraction, or keratometry. The average epithelial thickness map showed that the corneal epithelium was thicker inferiorly than superiorly (5.9 μm at the 3-mm radius,  $P < .001$ ) and thicker nasally than temporally (1.3 μm at the 3-mm radius,  $P < .001$ ). The location of the thinnest epithelium was displaced on average 0.33 mm temporally and 0.90 mm superiorly with reference to the corneal vertex.

**CONCLUSIONS**—Three-dimensional thickness mapping of the corneal epithelium demonstrated that the epithelial thickness is not evenly distributed across the cornea; the epithelium was significantly thicker inferiorly than superiorly and significantly thicker nasally than temporally with a larger inferosuperior difference than nasotemporal difference.

---

The human corneal epithelium has five to seven cell layers and an accepted central thickness of approximately 50 to 52 μm.<sup>1</sup> Bowman's layer, a dense collagenous layer approximately 8 to 10 μm thickness lies between the epithelium and stroma. The anterior margin of Bowman's

---

Correspondence: Dan Z. Reinstein, MD, MA(Cantab), FRCSC, London Vision Clinic, 8 Devonshire Pl, London W1G 6HP, United Kingdom. Tel: 44 207 224 1005; Fax: 44 207 224 1055; E-mail: dzt@londonvisionclinic.com.  
Drs Reinstein, Silverman, and Coleman have a proprietary interest in the Artemis technology (Ultralink LLC, St Petersburg, Fla) through patents administered by the Cornell Research Foundation, Ithaca, NY. The remaining authors have no proprietary or financial interest in the materials presented herein.

Prepared in part as fulfillment of the requirements for Dr Reinstein's doctoral thesis, University of Cambridge.

Some aspects of this study were presented at the American Academy of Ophthalmology Annual Meeting; November 11-14, 2006; Las Vegas, Nev.

layer presents a sharp interface with the lamina densa of the basement membrane of the overlying epithelium.<sup>2</sup> The corneal epithelium is a highly active, self-renewing layer; a complete turnover occurs in approximately 5 to 7 days.<sup>3</sup> Despite this high turnover rate, the epithelium must maintain the same thickness profile over time to maintain corneal power and, hence, ocular refraction. The epithelial thickness profile can affect the total corneal power because it determines the shape of the air-tear film interface, but also because of the difference in refractive index between epithelium and stroma (1.401 versus 1.377).<sup>4</sup> It has been calculated that the epithelium accounts for an average of 1.03 diopters of corneal power at the central 2-mm diameter zone.<sup>5</sup> We previously demonstrated how the epithelial thickness profile varies enough to be a significant factor in the accuracy of corneal refractive surgery.<sup>6</sup> Knowledge of the epithelial thickness profile and how it may change after corneal surgery could positively contribute to the accuracy of refractive corneal and intraocular lens surgery.

Different methods have been used to measure corneal epithelial thickness: optical coherence tomography (OCT),<sup>7,8</sup> confocal microscopy,<sup>9,10</sup> optical pachymetry,<sup>11</sup> and through focusing confocal microscopy.<sup>12</sup> All of these studies measured average central epithelial thickness. Some studies also provided epithelial thickness measurements in the peripheral cornea, but the number of points measured in the periphery was limited.<sup>11-13</sup>

High-frequency ultrasound provides sufficient resolution to resolve the cornea and its constituent layers, including the epithelium. The sharp anatomic discontinuity and density change between the epithelium and Bowman's layer results in a high-amplitude reflection at the epithelial-Bowman's layer junction. Although the cornea has evolved to minimize abrupt optical refractive changes between layers to prevent internal reflections, this is not the case for ultrasound. We previously described the use of very high-frequency (VHF) digital ultrasound to measure corneal epithelium,<sup>6</sup> with the first confirmed measurement of the epithelium of the cornea in vivo using a prototype rectilinear VHF digital ultrasound scanning system in 1993.<sup>14</sup> We demonstrated that acoustic interfaces detected were indeed located spatially at the epithelial surface and the interface between epithelial cells and the surface of Bowman's layer.<sup>15</sup> We also reported the first high-precision VHF three-dimensional epithelial thickness mapping system<sup>16</sup>; VHF digital ultrasound is, to date, the only published method measuring the corneal epithelial thickness profile continuously over a large area. Very high-frequency digital ultrasound technology has gradually improved both in precision and area of acquisition. The repeatability of epithelial thickness measurements in 10 consecutive examinations of 1 eye using the Artemis 1 VHF digital ultrasound arc-scanner (Ultralink LLC, St Petersburg, Fla) has been shown to be <1.30  $\mu\text{m}$  within an 8-mm diameter, with a central repeatability of 0.50  $\mu\text{m}$ .<sup>6</sup> The Artemis 1 is a commercial prototype, and further development is currently being undertaken by ArcScan Inc, Evergreen, Colo.

The purpose of this study was to characterize the thickness profile of the corneal epithelium in a population of normal eyes with no ocular pathology other than refractive error.

## PATIENTS AND METHODS

This retrospective, non-comparative case series is from a population of patients seeking refractive surgery at the London Vision Clinic between January 2003 and December 2005. A complete ocular examination was performed to screen for corneal abnormalities and determine patient candidacy for refractive surgery. Patients with ocular pathologies such as keratoconus, corneal scars, corneal dystrophies, and previous ocular surgery were excluded. The preoperative assessment of all patients included manifest refraction, logMAR best spectacle-corrected visual acuity (CSV-1000; Vector Vision Inc, Greenville, Ohio), and cycloplegic refraction using one drop of Tropicamide 1% (Alcon Laboratories UK Ltd, Herts, England). Topography and keratometry were assessed using the Orbscan II (Bausch & Lomb, Salt Lake

City, Utah). Dynamic pupillometry was carried out using the Procyon P2000 pupillometer (Procyon Instruments, London, England). Wavefront assessment was performed using the WASCA aberrometer (Carl Zeiss Meditec AG, Jena, Germany). Single-point, hand-held corneal thickness was measured with the Corneo-Gage Plus (50 MHz) ultrasound pachymeter (Sonogage, Cleveland, Ohio) by determining the minimum of 10 consecutive central corneal measurements. Three-dimensional epithelial thickness for the central 8- to 10-mm corneal diameter was obtained using the Artemis 1 technology.

Patients included in this study met the following inclusion criteria: patients whose corneal thickness might not be sufficient to perform LASIK based on manual corneal thickness measurements (ie, the residual stromal thickness predicted was  $<260\ \mu\text{m}$ ), high myopic patients, patients with a higher chance of requiring retreatment regardless of corneal thickness (high myopia or high cylinder), and patients selected at random from our refractive surgical candidates to broaden the distribution of refraction.

A written informed consent was obtained from all patients. The study adhered to the tenets of the Declaration of Helsinki and was performed in accordance with an Institutional Review Board approved protocol.

### Artemis VHF Digital Ultrasound Arc-scanning

Artemis VHF digital ultrasound was carried out using an ultrasonic standoff medium, and so provides the advantages of immersion scanning (eg, the tear-film is not incorporated in the corneal or epithelial thickness measurement, and has no physical contact of the transducer with the cornea). When seated, the patient positioned his/her chin and forehead into a headrest while placing the eye in a soft rimmed eye cup. Warm sterile normal saline ( $33^{\circ}\text{C}$ ) was filled into the darkened scanning chamber. The patient fixates on a narrowly focused aiming beam, which is coaxial with the infrared camera, the corneal vertex, and the center of rotation of the scanning system. The technician adjusts the center of rotation of the system until it is coaxial with the corneal vertex. In this manner, the position of each scan plane is maintained about a single point on the cornea and corneal mapping is, therefore, centered on the corneal vertex. A speculum is not required as patients find it comfortable to open the eye without blinking in the warm saline bath, and voluntary elevation of the upper lid produces exposure of the central 10 mm of cornea in virtually all patients. Performing a three-dimensional scan set with the Artemis 1 takes approximately 2 to 3 minutes per eye.

A broadband 50 MHz VHF ultrasound transducer (bandwidth approximately 10 to 60 MHz) is swept by a reverse arc high-precision mechanism to acquire B-scans as arcs that follow the surface contour of anterior or posterior segment structures of interest. The Artemis possesses a unique scan-arc adjustment mechanism to enable maximum perpendicularity (and signal-to-noise ratio) to be obtained for scanning any of the different curvatures within the globe (ie, cornea, iris plane, and retina). The resolution of the system is  $21\ \mu\text{m}$  whereas the precision of measurement varies according to position within the cornea, with  $0.5\ \mu\text{m}$  at the center and  $<1.3\ \mu\text{m}$  peripherally.<sup>6</sup> This means that if the epithelium being measured is at least  $21\ \mu\text{m}$  thick, the front and back surfaces will produce distinct echo peaks on the I-scan, allowing that layer to be measured with  $\sim 1\ \mu\text{m}$  precision.

### Three-dimensional Epithelial Pachymetric Topography

For three-dimensional scan sets, the scan sequence consisted of four meridional B-scans at  $45^{\circ}$  intervals. Each scan sweep took about 0.25 seconds and consisted of 128 scan lines or pulse echo vectors. During the acquisition of each scan, data were converted (in near real-time) to a B-scan displayed on the computer screen. Each B-scan reveals information regarding centration, ranging, and eye movements that may have occurred during the scan sweep. The

examiner either accepted or chose to repeat a particular meridional sweep before proceeding to the next. Ultrasound data were digitized and stored. The digitized ultrasound data were then transformed using patented Cornell University (Ithaca, NY) digital signal processing technology, which includes autocorrelation of back surface curvatures to center and align the meridional scans. A speed of sound constant of 1640 m/s was used.

Thickness profiles were calculated based on data from four meridional B-scans, comprised of eight semi-meridians. A linear polar/radial interpolation function was used to interpolate among scan meridians to produce a Cartesian matrix over a 10-mm diameter in 0.1-mm steps. This is our standard scanning protocol as it provides sufficiently high density of information in the central cornea with lower density of information in the periphery where it is less needed. Thickness maps of the epithelium were produced for each eye and plotted for the 10-mm diameter measured using DeltaGraph v5.0 (SPSS Inc, Richmond, Calif). Surface fill plots X, Y, and Z were employed to display epithelial thickness data on a color scale. A Cartesian 1-mm grid was superimposed with the origin centered at the corneal vertex, which closely approximates the visual axis.

### Statistical Analysis

Descriptive statistics (average, minimum, maximum, standard deviation, and range) were calculated for each point in the 10×10-mm Cartesian matrix across eyes. These statistics were calculated for right eyes only, for left eyes only, and for all eyes using vertical mirrored symmetry superimposition; epithelial thickness values for left eyes were reflected in the vertical axis and superimposed onto the right eye values so that nasal/temporal characteristics could be combined. The resultant matrices were plotted as surface fill plots X, Y, and Z to represent the point-by-point average, standard deviation, minimum, maximum, and range of the population. Qualitative assessment of individual variability within corneas and across the population was performed. The Kolmogorov-Smirnov test was performed to test for non-normality of the epithelial thickness data at the corneal vertex. Student paired *t* test was performed to compare the epithelial thickness at the corneal vertex between right and left eyes. Quantitative assessment of the difference in epithelial thickness between the center and periphery of the cornea was performed (using mirrored left eyes) by isolating the descriptive statistics at the corneal vertex and points at a 3-mm radius inferiorly, superiorly, nasally, and temporally. The differences between the 3-mm superior, 3-mm inferior, and corneal vertex epithelial thickness, and between 3-mm nasal, 3-mm temporal, and corneal vertex epithelial thickness were calculated. Student paired *t* tests were carried out to identify any statistically significant differences in epithelial thickness between the 3-mm superior, 3-mm inferior, and corneal vertex epithelial thickness, and between 3-mm nasal, 3 mm-temporal, and corneal vertex epithelial thickness. The point location of the thinnest epithelium was determined for each eye (using mirrored left eyes), and the average and standard deviation of the X and Y coordinates of the thinnest point were calculated. The standard deviation of epithelial thickness within the central 3-, 5-, and 7-mm diameter zones was determined for each eye to represent the within-eye variation of epithelial thickness. The average and standard deviation of the within-eye variation were found, and the distribution of the within-eye variation was plotted.

Linear regression analysis was performed to seek possible correlations between corneal vertex epithelial thickness and age, spherical equivalent refraction, and average keratometry. Descriptive statistics, comparative statistics, and linear regression were performed in Microsoft Excel 2003 (Microsoft Corp, Redmond, Wash). The Kolmogorov-Smirnov test for non-normality was performed using the online form at [http://www.physics.csbsju.edu/stats/KS-test.n.plot\\_form.html](http://www.physics.csbsju.edu/stats/KS-test.n.plot_form.html). A *P* value of <.05 was considered to be statistically significant.

## RESULTS

During the study period, 110 eyes of 56 patients (55 right and 55 left eyes) were recruited. The other eyes of 2 patients were excluded from the study due to corneal scar. Study population included 74% Caucasian, 17% East Indian, 5% East Asian, and 4% Black patients. Population mean age was  $38.4 \pm 12.0$  years (median: 36.1 years, range: 20.5 to 73.5 years). Mean refraction was  $-6.04 \pm 3.58$  diopters (D) sphere (range:  $-12.00$  to  $+6.00$  D), and  $-1.51 \pm 1.30$  D (range: 0.00 to  $-5.00$  D) cylinder. Although the refraction was biased toward high myopes, the population was considered normal as all patients were free of ocular pathology other than refractive error.

Mean ( $\pm$ standard deviation) corneal vertex epithelial thickness for all eyes was  $53.4 \pm 4.6$   $\mu\text{m}$  (95% confidence interval: 52.5% to 54.3%) (Table 1). Corneal vertex epithelial thickness ranged from 43.5 to 63.6  $\mu\text{m}$  for all eyes. Mean ( $\pm$ standard deviation) corneal vertex epithelial thickness was  $53.1 \pm 4.5$   $\mu\text{m}$  for right eyes and  $53.7 \pm 4.7$   $\mu\text{m}$  for left eyes. No statistically significant difference between the mean corneal vertex epithelial thickness of right and left eyes was noted ( $P=.497$ ). No statistical evidence of non-normality of the corneal vertex epithelial thickness within the population using the Kolmogorov-Smirnov test for non-normality was noted ( $P=.48$ ).

The average epithelial thickness maps (Fig 1, column 1) showed the corneal epithelium was thinner in the superior cornea and thicker in the inferior cornea. The mean ( $\pm$ standard deviation) of the epithelial thickness at locations 3-mm superior, inferior, nasal, and temporal of the corneal vertex are summarized in Figure 2. The 3-mm superior epithelium was 5.7- $\mu\text{m}$  thinner than the 3-mm inferior epithelium ( $P<.001$ ). The corneal vertex epithelium was 5.4- $\mu\text{m}$  thinner than the 3-mm inferior epithelial thickness ( $P<.001$ ). Although the corneal vertex epithelium was 0.3- $\mu\text{m}$  thicker than the 3-mm superior epithelium, this difference was not statistically significant ( $P=.570$ ).

The mirrored average epithelial thickness map (see Fig 1, row 1, column 1) showed that the corneal epithelium was thicker nasally than temporally. The 3-mm temporal epithelium was 1.2- $\mu\text{m}$  thinner than the 3-mm nasal epithelium ( $P<.001$ ). The corneal vertex epithelium was 1.6- $\mu\text{m}$  thinner than the 3-mm nasal epithelial thickness ( $P<.001$ ). Although the corneal vertex epithelium was 0.4- $\mu\text{m}$  thinner than the 3-mm temporal epithelium, this difference was not statistically significant ( $P=.325$ ).

Figure 3 shows the epithelial thickness profile plotted for 15 eyes of the population selected at random using Microsoft Excel's random number function. Although most eyes exhibited a pattern of thinner superior than inferior epithelium and thinner temporal than nasal epithelium (see Fig 3, patients 2, 5, and 15), there was variation in the corneal epithelial thickness between individual eyes; some eyes showed a thinner central epithelium and a thicker peripheral epithelium (see Fig 3, patient 12), and some eyes demonstrated a thicker central epithelium and thinner peripheral epithelium (see Fig 3, patient 4).

Maps of epithelial thickness standard deviation (see Fig 1, column 2) showed more variation in epithelial thickness in the inferior region. The superonasal region demonstrated the least variation. Maps of the minimum epithelial thickness (see Fig 1, column 3) demonstrated the thinnest epithelium within the study population to be in the superotemporal region. The thinnest superior epithelium within the study population was 36  $\mu\text{m}$ , whereas the thinnest inferior epithelium in the study population was 47  $\mu\text{m}$ , highlighting the difference between the superior and inferior epithelial thickness. Maps of the maximum epithelial thickness (see Fig 1, column 4) demonstrated that the thickest epithelium within the study population was found in the inferior region. The thickest superior epithelium in the study population was 60  $\mu\text{m}$ , whereas the thickest inferior epithelium within the study population was 68  $\mu\text{m}$ , again highlighting the



difference between the superior and inferior epithelial thickness. Maps of the range of epithelial thickness (see Fig 1, column 5) demonstrated the largest range in epithelial thickness to be in the superotemporal region and the smallest range in the inferonasal region.

Analysis of the thinnest epithelial point within the central 5 mm of the cornea found that the mean ( $\pm$ standard deviation) thinnest epithelial point was displaced 0.33 mm ( $\pm$ 1.08) temporally and 0.90 mm ( $\pm$ 0.96) superiorly with reference to the corneal vertex (Fig 4).

The within-eye variation of epithelial thickness for the central 3-, 5-, and 7-mm diameter zones is described in Table 2. The average within-eye variation of epithelial thickness increased as the analysis zone diameter increased (Fig 5). The mean ( $\pm$ standard deviation) within-eye variation of epithelial thickness was  $1.50\pm 0.68$   $\mu$ m for the central 3-mm zone,  $2.19\pm 0.91$   $\mu$ m for the central 5-mm zone, and  $2.84\pm 1.02$   $\mu$ m for the central 7-mm zone.

No statistically significant correlation between corneal vertex epithelial thickness and spherical equivalent refraction ( $P=.81$ ,  $r^2<0.001$ ) was noted, nor between corneal vertex epithelial thickness and central keratometry ( $P=.86$ ,  $r^2=0.0003$ ). No correlation between corneal vertex epithelial thickness and age was noted ( $P=.44$ ,  $r^2=0.006$ ), nor 3-mm inferior epithelial thickness and age ( $P=.29$ ,  $r^2=0.01$ ), nor 3-mm superior epithelial thickness and age ( $P=.47$ ,  $r^2=0.01$ ). A statistically significant trend for the 3-mm superior epithelium to become thinner with increasing age  $>45$  years ( $P=.02$ ,  $r^2=0.17$ ) was seen; however, this was largely due to the superior epithelial thickness of one patient in the study. The correlation between 3-mm superior epithelium and age was not statistically significant if the two eyes of this patient were excluded from the analysis. No statistically significant difference in corneal vertex epithelial thickness between the over and under 45-year-old patients was noted ( $P=.100$ ).

## DISCUSSION

In this study, we characterized the corneal epithelial thickness profile over a 10-mm diameter area in a population of normal eyes. We found an average corneal vertex epithelial thickness of  $53.4\pm 4.6$   $\mu$ m. The epithelial thickness was found to follow a non-uniform pattern, with the 3-mm inferior epithelium 5.7  $\mu$ m thicker than the 3-mm superior epithelium and the 3-mm nasal epithelium 1.2  $\mu$ m thicker than the 3-mm temporal epithelium.

We previously described the signal processing strategies for measurement of epithelial thickness.<sup>15</sup> Two potential sources of uncertainty in ultrasound measurement of the thickness of the corneal epithelium are the epithelial speed of sound constant and the anatomic source of the echo we associate with the interface between the epithelium and Bowman's layer. Although the acoustic transmission properties of the whole cornea at 50 to 100 MHz have been investigated by Ye et al,<sup>17</sup> no data exist for speed of sound in the corneal epithelium alone. It is reasonable to assume that the epithelial speed of sound lies somewhere between 1640 m/s (the accepted value for the speed of sound of the cornea), and the lowermost limit of 1525 m/s (the speed of sound in normal saline at 33°C). This implausible worst-case value would lead to a 7% overestimate in epithelial thickness measurements made using 1640 m/s, leading to a systematic overestimate of about 3.5  $\mu$ m. One other ultrasonic phenomenon that could theoretically affect accuracy is dispersion. In dispersion, the speed of sound increases with increasing frequency within the same medium; however, dispersion at frequencies between 30 and 60 MHz is negligible. Therefore, speed of sound constant errors in epithelial thickness measurements are justifiably negligible. In addition, any such error would affect all measurements and would, therefore, have no effect on our findings regarding epithelial thickness distributions across the cornea.

Bowman's layer is approximately 8- $\mu$ m thick. As such, Bowman's layer would produce acoustic reflections from both its anterior interface with the epithelium and its posterior

interface with the stroma. The resolution of the system described in this study is 21  $\mu\text{m}$ ; therefore, individual echo signals from the front and back surface of Bowman's layer are not resolved and appear as a single reflection. We demonstrated that the acoustic impedance change at the front of Bowman's layer is six times greater than at the back of Bowman's layer; therefore, the energy maximum of the echo complex emitted by Bowman's layer will be, for all intents and purposes, located at the front surface interface of Bowman's layer with the epithelium.<sup>15</sup> Not only is the Bowman's echo uncertainty negligible, it is also systematic and consequently would not affect conclusions regarding the epithelial thickness distribution across the cornea. Ye et al<sup>17</sup> also report a frequency-dependent attenuation coefficient of 1.3 dB/mm at 50 MHz. This would translate to <1 dB attenuation over the full thickness of the cornea and a small fraction of a decibel over the epithelium. Thus, attenuation is of no practical significance in ultrasound biometry of the cornea at 50 MHz.

The patients recruited in our study represented a population of normal eyes, with a refraction biased toward high myopes. However, there was no statistically significant correlation between central epithelial thickness and spherical equivalent refraction ( $P=.81$ ,  $r^2=0.0006$ ). As a consequence, the point thickness data as well as the epithelial thickness profiles are likely to be representative of a true normal population.

Central corneal epithelial thickness has been previously measured with the reported values varying between  $48\pm 5 \mu\text{m}$ <sup>11</sup> and  $59.9\pm 5.9 \mu\text{m}$ <sup>18-21</sup> (Table 3). Using a rectilinear VHF digital ultrasound prototype, we found the central epithelial thickness in 20 normal eyes averaged within the central 3-mm diameter to be  $50.7\pm 3.7 \mu\text{m}$ .<sup>22</sup> The mean and standard deviation of corneal vertex epithelial thickness found in this study are consistent with previously reported values obtained by a variety of measurement techniques. Of the studies that investigated non-central epithelial thickness, all reported no differences between central and peripheral locations.<sup>11,23</sup> Pérez et al<sup>11</sup> measured epithelial thickness at four mid-peripheral and four peripheral locations in the vertical and horizontal meridians using a modified optical pachymeter and found that the epithelium was roughly uniform in thickness in the central 8 mm of the cornea. Using OCT (Humphrey systems; Zeiss-Humphrey, Dublin, Calif), Wang et al<sup>23</sup> measured epithelial thickness at intervals of  $10^\circ$  across a 10-mm zone of the horizontal meridian of the cornea and concluded that the epithelial thickness was constant along the horizontal. Patel et al,<sup>13</sup> using a tandem scanning confocal microscope (Tandem Scanning, Reston, Va), found no significant difference between central epithelial thickness and temporal epithelial thickness measured 2.5-mm nasal to the limbus. It is interesting to note that OCT and confocal microscopy have not found differences in epithelial thickness between central and peripheral corneal locations as were described in the present study. It would be interesting to perform a comparative study of the epithelial thickness profile across the central 10-mm diameter of the cornea using Artemis ultrasound, OCT, and confocal microscopy.

Simon et al<sup>5</sup> suggested that the epithelium does not form a layer of uniform thickness, which is in agreement with the findings in the present study. In that previous study, the power of the epithelium was calculated using corneal keratometry measurements with and without the epithelium; the measurements were performed for the central 2- and 3.6-mm diameter zones in 10 human eye bank eyes. The authors reported changes in corneal refractive power and, in particular, changes in both the power and axis of astigmatism. They suggested the change in astigmatism could be due to changes in epithelial thickness.

Further study may elicit the mechanisms underlying the non-uniform epithelial thickness profile found in our study population; in particular, why the epithelium was thinner superiorly than inferiorly. We originally suggested in 1994 that blinking and friction onto the cornea may regulate the corneal epithelial thickness profile.<sup>16</sup> During blinking, which occurs on average between 300 to 1500 times per hour,<sup>24</sup> the vertical traverse of the upper lid is much greater

than that of the lower lid. Doane<sup>25</sup> studied the dynamics of eyelid anatomy during blinking, and found that during a blink the descent of the upper eyelid reaches its maximum speed at about the time it crosses the visual axis. As a consequence, the eyelid might effectively be chafing the surface epithelium during blinking, with greater forces applied on the superior cornea than on the inferior cornea. This could explain why the epithelium was found to be thinner superiorly.

We also found that the temporal epithelium was thinner than the nasal epithelium. Further study is necessary to explain the reason behind this finding. We postulate that the friction on the cornea during lid closure is greater on the temporal cornea than on the nasal cornea as the outer canthus is higher than the inner canthus (mean intercanthal angle=3°), and the temporal portion of the lid higher than the nasal lid (mean upper lid angle=2.7°).<sup>26</sup>

The within-eye variation of epithelial thickness was found to increase centrifugally. Thus, the regularity of the epithelial thickness profile diminishes with increasing pupil size or corneal optical zone. Given the refractive contribution of the epithelium, this could play a role in the observed decrease in optical quality of vision with increasing pupil size. How the epithelial thickness profile changes induced by corneal refractive surgery influence the induction of higher order aberrations is the subject of further study.

The ability to characterize the epithelial thickness profile may help in various areas of ophthalmology; it may help further increase the accuracy of corneal refractive surgery as epithelial changes are known to play a role in refractive regression.<sup>27-34</sup> Modulation of the epithelial thickness within the cornea may contribute to changes in the overall refraction of the eye; use of topical corticosteroids after photorefractive keratectomy has been shown to produce hyperopic shifts in refraction, which are reversed once the corticosteroids are stopped.<sup>35</sup> If epithelial dynamics were found to follow a predictable pattern after refractive surgery, this knowledge could be used to improve the accuracy of outcomes.

Epithelial thickness profiles may also prove to be a useful diagnostic tool in screening for keratoconus as it is known that the epithelium thins over the region of the cone in keratoconus, sometimes leading to epithelial breakdown. We are currently investigating the epithelial thickness profiles of eyes with frank keratoconus and forme fruste keratoconus to attempt to subdivide forme fruste keratoconic eyes into 'true' and 'pseudo' keratoconic groups.

Knowledge of the corneal epithelial profile may also be of interest in the contact lens field. In orthokeratology, it is not yet fully understood whether the modification of corneal power is the result of epithelial thickness profile warpage or stromal surface warpage or both. Recent studies have demonstrated a change in corneal epithelial thickness following the wear of overnight refractive therapy rigid contact lenses, with a thinning of the epithelium centrally and a thickening of the epithelium in the periphery.<sup>7,20</sup>

Finally, an analysis of the shift in corneal power from before-to-after corneal refractive surgery may aid clinicians in determining the cause of regression in the refractive effect. Distinguishing epithelial from biomechanical causes of regression may be important in preventing destabilization of the corneal architecture (keratectasia) by retreatment surgery.

To our knowledge, this is the first study to describe the full corneal characteristics of epithelial pachymetric topography in the human cornea. Three-dimensional thickness mapping of the corneal epithelium demonstrated that epithelial thickness is not evenly distributed across the cornea. Knowledge of the epithelial thickness profile in the normal cornea should help in understanding corneal refractive surgical accuracy, as well as improving the diagnosis in corneal diseases.



## Acknowledgements

Supported in part by National Institutes of Health (NIH), Bethesda, Md, grant EB000238 and the Dyson Foundation.

## References

1. Hogan, MJ.; Alvarado, JA.; Weddell, JE. *Histology of the Human Eye*. Philadelphia, Pa: Saunders Publishing; 1971.
2. Kobayashi A, Yokogawa H, Sugiyama K. In vivo laser confocal microscopy of Bowman's layer of the cornea. *Ophthalmology* 2006;113:2203–2208. [PubMed: 17157133]
3. Hanna C, O'Brien JE. Cell production and migration in the epithelial layer of the cornea. *Arch Ophthalmol* 1960;64:536–539. [PubMed: 13711262]
4. Patel S, Marshall J, Fitzke FW III. Refractive index of the human corneal epithelium and stroma. *J Refract Surg* 1995;11:100–105. [PubMed: 7634138]
5. Simon G, Ren Q, Kervick GN, Parel JM. Optics of the corneal epithelium. *Refract Corneal Surg* 1993;9:42–50. [PubMed: 8481372]
6. Reinstein DZ, Silverman RH, Raevsky T, Simoni GJ, Lloyd HO, Najafi DJ, Rondeau MJ, Coleman DJ. Arc-scanning very high-frequency digital ultrasound for 3D pachymetric mapping of the corneal epithelium and stroma in laser in situ keratomileusis. *J Refract Surg* 2000;16:414–430. [PubMed: 10939721]
7. Wang J, Fonn D, Simpson TL, Sorbara L, Kort R, Jones L. Topographical thickness of the epithelium and total cornea after overnight wear of reverse-geometry rigid contact lenses for myopia reduction. *Invest Ophthalmol Vis Sci* 2003;44:4742–4746. [PubMed: 14578394]
8. Feng Y, Simpson TL. Comparison of human central cornea and limbus in vivo using optical coherence tomography. *Optom Vis Sci* 2005;82:416–419. [PubMed: 15894917]
9. Ladage PM, Yamamoto K, Ren DH, Li L, Jester JV, Petroll WM, Cavanagh HD. Effects of rigid and soft contact lens daily wear on corneal epithelium, tear lactate dehydrogenase, and bacterial binding to exfoliated epithelial cells. *Ophthalmology* 2001;108:1279–1288. [PubMed: 11425688]
10. Møller-Pedersen T, Vogel M, Li HF, Petroll WM, Cavanagh HD, Jester JV. Quantification of stromal thinning, epithelial thickness, and corneal haze after photorefractive keratectomy using in vivo confocal microscopy. *Ophthalmology* 1997;104:360–368. [PubMed: 9082257]
11. Pérez JG, Méijome JM, Jalbert I, Sweeney DF, Erickson P. Corneal epithelial thinning profile induced by long-term wear of hydrogel lenses. *Cornea* 2003;22:304–307. [PubMed: 12792471]
12. Li HF, Petroll WM, Moller-Pedersen T, Maurer JK, Cavanagh HD, Jester JV. Epithelial and corneal thickness measurements by in vivo confocal microscopy through focusing (CMTF). *Curr Eye Res* 1997;16:214–221. [PubMed: 9088737]
13. Patel SV, McLaren JW, Hodge DO, Bourne WM. Confocal microscopy in vivo in corneas of long-term contact lens wearers. *Invest Ophthalmol Vis Sci* 2002;43:995–1003. [PubMed: 11923239]
14. Reinstein DZ, Silverman RH, Trokel SL, Rondeau MJ, Coleman DJ. High-frequency ultrasound three dimensional pachymetry and keratometry of the cornea. Presented at: Association for Research in Vision and Ophthalmology. 1993
15. Reinstein DZ, Silverman RH, Coleman DJ. High-frequency ultrasound measurement of the thickness of the corneal epithelium. *Refract Corneal Surg* 1993;9:385–387. [PubMed: 8241045]
16. Reinstein DZ, Silverman RH, Trokel SL, Coleman DJ. Corneal pachymetric topography. *Ophthalmology* 1994;101:432–438. [PubMed: 8127563]
17. Ye SG, Harasiewicz KA, Pavlin CJ, Foster FS. Ultrasonic characterization of normal ocular tissue in the frequency range from 50 MHz to 100. MHz. *IEEE Transactions on Ultrasonics, Ferroelectrics and Frequency Control* 1995;42:8–14.
18. Wang J, Thomas J, Cox I, Rollins A. Noncontact measurements of central corneal epithelial and flap thickness after laser in situ keratomileusis. *Invest Ophthalmol Vis Sci* 2004;45:1812–1816. [PubMed: 15161844]
19. Wirbelauer C, Pham DT. Monitoring corneal structures with slitlamp-adapted optical coherence tomography in laser in situ keratomileusis. *J Cataract Refract Surg* 2004;30:1851–1860. [PubMed: 15342046]

20. Haque S, Fonn D, Simpson T, Jones L. Corneal and epithelial thickness changes after 4 weeks of overnight corneal refractive therapy lens wear, measured with optical coherence tomography. *Eye Contact Lens* 2004;30:189–193. [PubMed: 15499246]
21. Møller-Pedersen T, Li HF, Petroll WM, Cavanagh HD, Jester JV. Confocal microscopic characterization of wound repair after photorefractive keratectomy. *Invest Ophthalmol Vis Sci* 1998;39:487–501. [PubMed: 9501858]
22. Reinstein DZ, Silverman RH, Rondeau MJ, Coleman DJ. Epithelial and corneal thickness measurements by high-frequency ultrasound digital signal processing. *Ophthalmology* 1994;101:140–146. [PubMed: 8302547]
23. Wang J, Fonn D, Simpson TL. Topographical thickness of the epithelium and total cornea after hydrogel and PMMA contact lens wear with eye closure. *Invest Ophthalmol Vis Sci* 2003;44:1070–1074. [PubMed: 12601031]
24. Bentivoglio AR, Bressman SB, Cassetta E, Carretta D, Tonali P, Albanese A. Analysis of blink rate patterns in normal subjects. *Mov Disord* 1997;12:1028–1034. [PubMed: 9399231]
25. Doane MG. Interactions of eyelids and tears in corneal wetting and the dynamics of the normal human eyeblink. *Am J Ophthalmol* 1980;89:507–516. [PubMed: 7369314]
26. Young G, Hunt C, Covey M. Clinical evaluation of factors influencing toric soft contact lens fit. *Optom Vis Sci* 2002;79:11–19. [PubMed: 11828894]
27. Reinstein DZ, Silverman RH, Sutton HF, Coleman DJ. Very high-frequency ultrasound corneal analysis identifies anatomic correlates of optical complications of lamellar refractive surgery: anatomic diagnosis in lamellar surgery. *Ophthalmology* 1999;106:474–482. [PubMed: 10080202]
28. Gauthier CA, Epstein D, Holden BA, Tengroth B, Fagerholm P, Hamberg-Nyström H, Sievert R. Epithelial alterations following photorefractive keratectomy for myopia. *J Refract Surg* 1995;11:113–118. [PubMed: 7634140]
29. Gauthier CA, Holden BA, Epstein D, Tengroth B, Fagerholm P, Hamberg-Nyström H. Role of epithelial hyperplasia in regression following photorefractive keratectomy. *Br J Ophthalmol* 1996;80:545–548. [PubMed: 8759267]
30. Lohmann CP, Reischl U, Marshall J. Regression and epithelial hyperplasia after myopic photorefractive keratectomy in a human cornea. *J Cataract Refract Surg* 1999;25:712–715. [PubMed: 10330651]
31. Philipp WE, Speicher L, Göttinger W. Histological and immunohistochemical findings after laser in situ keratomileusis in human corneas. *J Cataract Refract Surg* 2003;29:808–820. [PubMed: 12686254]
32. Erie JC, Patel SV, McLaren JW, Ramirez M, Hodge DO, Maguire LJ, Bourne WM. Effect of myopic laser in situ keratomileusis on epithelial and stromal thickness: a confocal microscopy study. *Ophthalmology* 2002;109:1447–1452. [PubMed: 12153794]
33. Spadea L, Fasciani R, Necozone S, Balestrazzi E. Role of the corneal epithelium in refractive changes following laser in situ keratomileusis for high myopia. *J Refract Surg* 2000;16:133–139. [PubMed: 10766381]
34. Reinstein DZ, Ameline B, Puech M, Montefiore G, Laroche L. VHF digital ultrasound three-dimensional scanning in the diagnosis of myopic regression after corneal refractive surgery. *J Refract Surg* 2005;21:480–484. [PubMed: 16209446]
35. O’Brart DP, Lohmann CP, Klonos G, Corbett MC, Pollock WS, Kerr-Muir MG, Marshall J. The effects of topical corticosteroids and plasmin inhibitors on refractive outcome, haze, and visual performance after photorefractive keratectomy. A prospective, randomized, observer-masked study. *Ophthalmology* 1994 Sep;101(9):1565–74. [PubMed: 7522315]

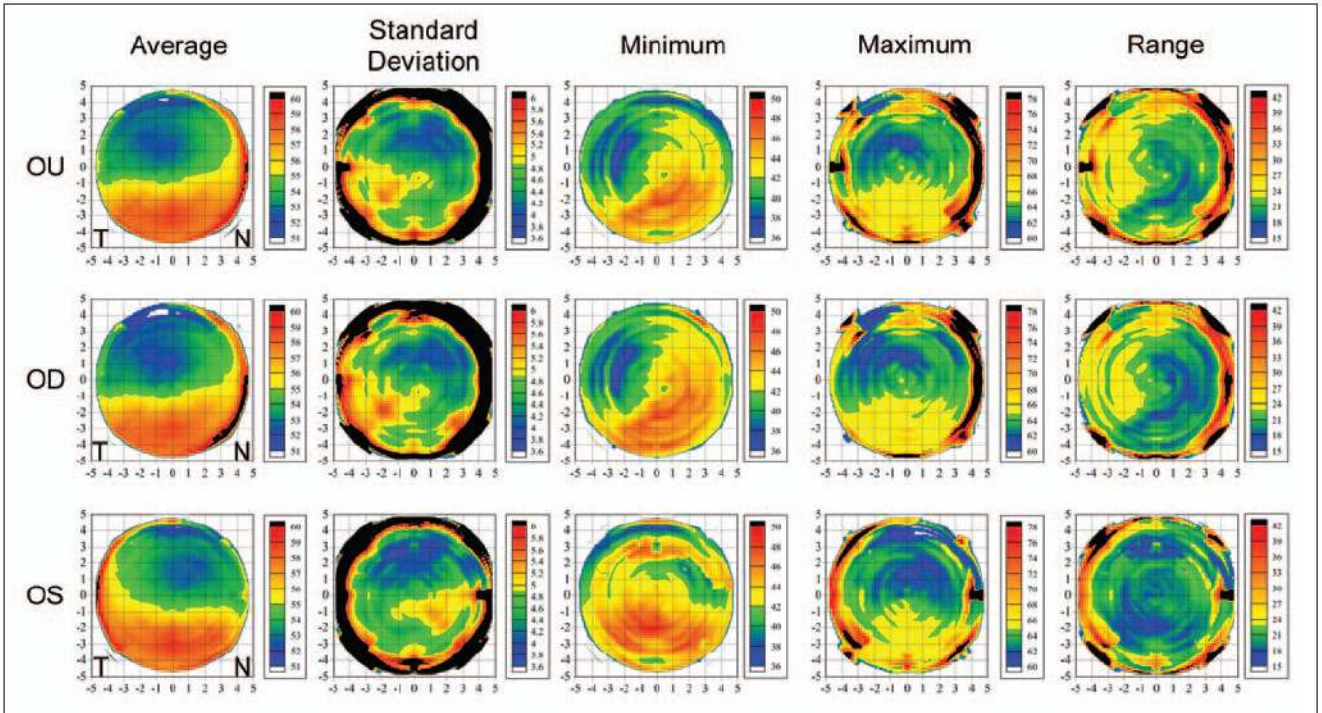


**Figure 1.** Topographical map of descriptive statistics of epithelial thickness for the population. The color scale represents epithelial thickness ( $\mu\text{m}$ ). A Cartesian 1-mm grid is superimposed with the origin at the visual axis. Row 1 includes all eyes with left eyes mirrored (positive X-values represent the nasal epithelium and negative values represent the temporal epithelium). Row 2 includes only right eyes, and Row 3 includes only left eyes. Point-by-point average maps are shown in column 1, point-by-point standard deviation maps are shown in column 2, point-by-point minimum maps are shown in column 3, point-by-point maximum maps are shown in column 4, and point-by-point range maps are shown in column 5.

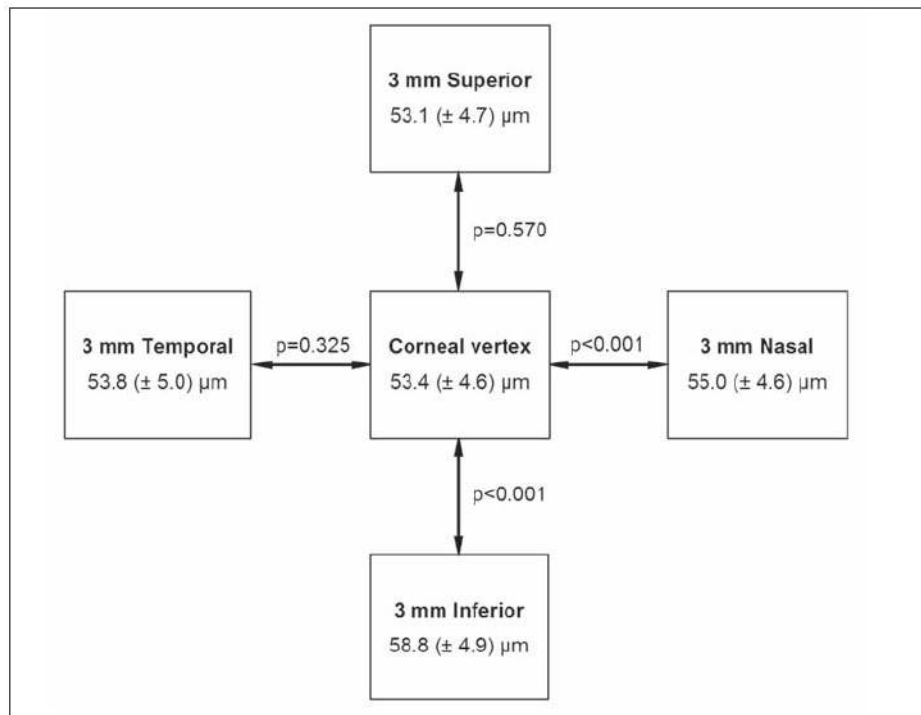


**Figure 2.** Mean ( $\pm$ standard deviation) central, nasal, temporal, superior, and inferior epithelial thickness at the 3-mm radius for all eyes. Student *t* test *P* values are displayed between central and peripheral locations to indicate the statistically significant differences.



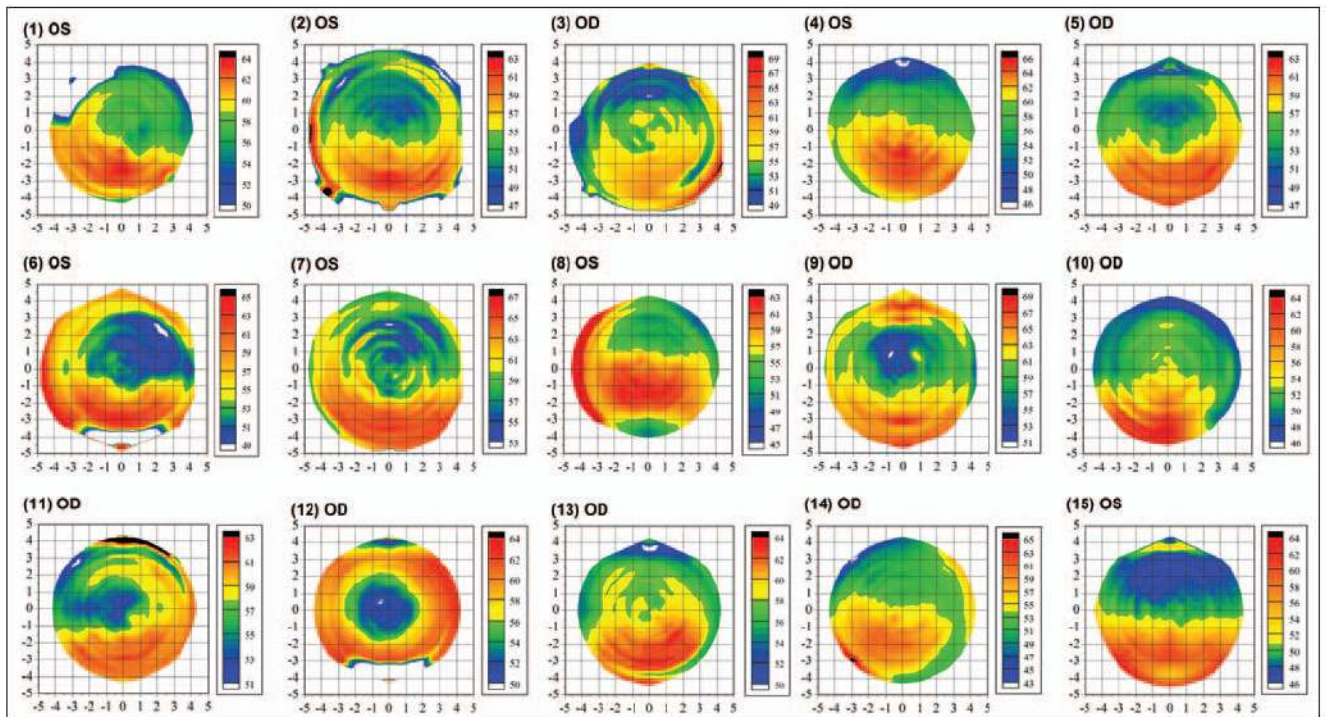


**Figure 3.**

**A)** Normalized epithelial thickness maps for 15 individual eyes. Epithelial thickness maps of 15 randomly selected eyes plotted with an identical color scale representing the epithelial thickness ( $\mu\text{m}$ ). A Cartesian 1-mm grid is superimposed with the origin at the corneal vertex.

**B)** Absolute epithelial thickness maps for 15 individual eyes. Epithelial thickness maps of 15 randomly selected eyes each plotted with an individual color scale representing the epithelial thickness ( $\mu\text{m}$ ). A Cartesian 1-mm grid is superimposed with the origin at the corneal vertex.



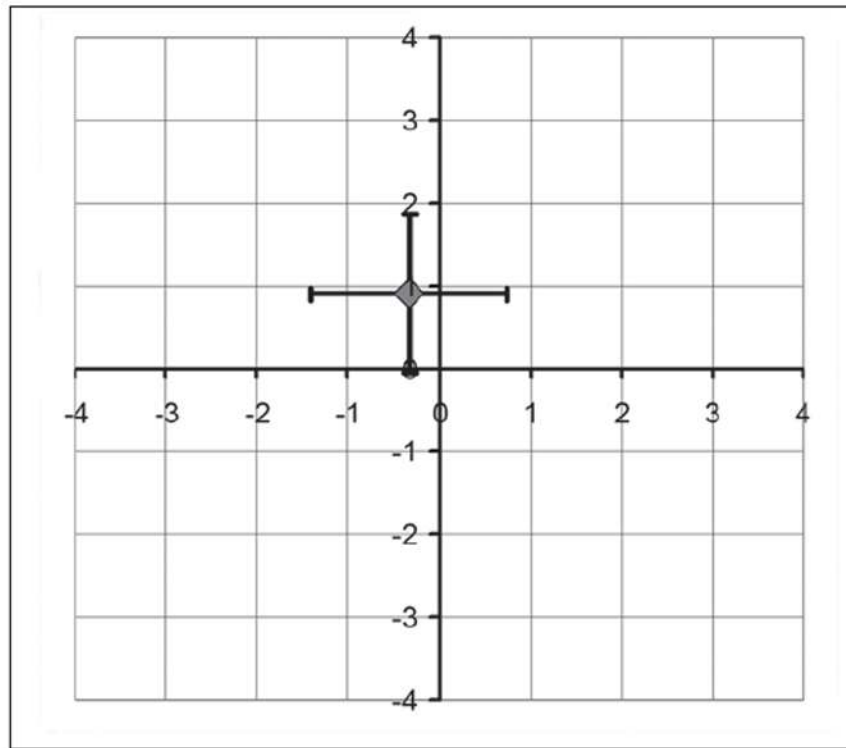


**Figure 4.** Average location of the thinnest epithelium within the central 5 mm of the cornea. The diamond represents the average location of the thinnest epithelium for all eyes tested, and the error bars represent one standard deviation in the X and Y directions.

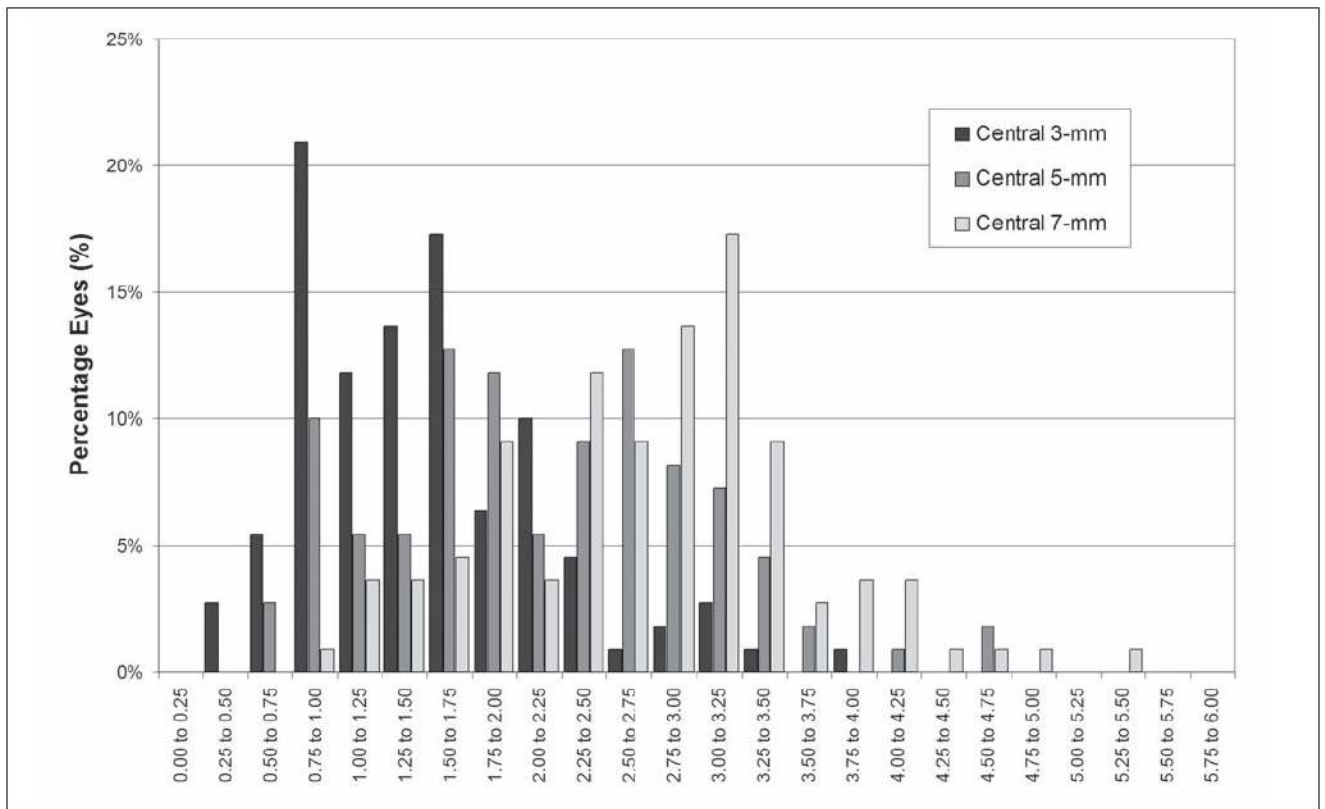


**Figure 5.** Histogram of within-eye variation of epithelial thickness for the central 3-, 5-, and 7-mm zones. The X axis represents the within-eye variation of epithelial thickness for the central 3-mm (black bars), 5-mm (gray bars), and 7-mm (light gray bars) diameter zones with intervals of 0.25 μm. Each bar represents the percentage of eyes with the within-eye variation of epithelial thickness for that 0.25-μm interval.

**TABLE 1**

Corneal Vertex Epithelial Thickness Measured With Artemis VHF Digital Ultrasound  
 Corneal Vertex Epithelial Thickness ( $\mu\text{m}$ )

	<b>All Eyes (N=110)</b>	<b>Right Eyes (n=55)</b>	<b>Left Eyes (n=55)</b>
Mean $\pm$ SD	53.4 $\pm$ 4.6	53.1 $\pm$ 4.5	53.7 $\pm$ 4.7
Minimum	43.5	43.5	44.0
Maximum	63.6	63.6	63.2
Range	20.1	20.1	19.2

**TABLE 2**

Epithelial Thickness Within the Central Diameter Zones (Within-eye Variation)

Within-eye Variation of Epithelial Thickness ( $\mu\text{m}$ )

	Diameter Zone		
	3 mm	5 mm	7 mm
Mean ( $\pm$ SD)	1.50 $\pm$ 0.68	2.16 $\pm$ 0.86	2.77 $\pm$ 0.86
Minimum	0.36	0.63	0.77
Maximum	3.78	4.60	5.43
Range	3.42	3.97	4.66

**TABLE 3**

## Central Epithelial Thickness Measurement Reported in the Literature

Investigator	No. of Eyes	Epithelial Thickness (Mean±SD) (μm)	Method of Measurement
Feng & Simpson <sup>8</sup>	20	58.4±2.5 (RE) 58.5±2.5 (LE)	Optical coherence tomography
Pérez et al <sup>11</sup>	36	48.0±5.0	Optical pachymeter
Li et al <sup>12</sup>	14	50.6±3.9	Confocal microscopy through focusing
Patel et al <sup>13</sup>	19	49.0±5.5	Confocal microscopy
Reinstein et al <sup>14</sup>	20	50.7±3.7 (RE) 50.3±3.4 (LE)	Rectilinear scanning VHF digital ultrasound
Wang et al <sup>18</sup>	28	59.9±5.9	Optical coherence tomography
Wirbelauer et al <sup>19</sup>	25	57.7±.7	Optical coherence tomography
Haque et al <sup>20</sup>	66	52.0±2.6 (RE) 52.0±3.1 (LE)	Optical coherence tomography
Møller-Pederson et al <sup>21</sup>	34	51.0±4.0	Confocal microscopy through focusing
Current study	110	53.1±4.5 (RE) 53.7±4.7 (LE)	Arc scanning VHF digital ultrasound

RE = right eye, LE = left eye, VHF = very high-frequency